JACS
JOURNAL OF THE AMERICAN CHEMICAL SOCIETY
Communication
pubs.acs.org/JACS

Activation of H_2 over the Ru−Zn Bond in the Transition Metal−Lewis Acid Heterobimetallic Species $[Ru(IPr)_2(CO)ZnEt]^+$

Ian M. Riddlestone,[#] Nasir A. Rajabi,[§] John P. Lowe,[#] Mary F. Mahon,[#] Stuart A. Macgregor,*[,§] and Michael K. Whittlesey*[,#]

[#]Department of Chemistry, University of Bath, Claverton Down, Bath BA2 7AY, U.K.
[§]Institute of Chemical Sciences, Heriot-Watt University, Edinburgh EH14 4AS, U.K.

Supporting Information

ABSTRACT: Reaction of $[Ru(IPr)_2(CO)H]BAr^F_4$ with $ZnEt_2$ forms the heterobimetallic species $[Ru(IPr)_2(CO)ZnEt]BAr^F_4$ (**2**), which features an unsupported Ru-Zn bond. **2** reacts with H_2 to give $[Ru(IPr)_2(CO)(\eta^2\text{-}H_2)(H)_2ZnEt]BAr^F_4$ (**3**) and $[Ru(IPr)_2(CO)(H)_2ZnEt]BAr^F_4$ (**4**). DFT calculations indicate that H_2 activation at **2** proceeds via oxidative cleavage at Ru with concomitant hydride transfer to Zn. **2** can also activate hydridic E-H bonds (E = B, Si), and computed mechanisms for the facile H/H exchange processes observed in **3** and **4** are presented.

Metal−ligand cooperativity is a widely used strategy for the activation and catalytic transformation of small molecules.[1] Many such systems are predicated on transition metal−-Lewis base (TM-LB) combinations,[2,3] as well as those featuring electronically flexible ligand scaffolds, exemplified by Milstein's (de)aromatization approach.[4] More recently, TM-LA (LA = Lewis acid) cooperativity has (re)emerged,[5] with reports of H_2 cleavage,[6] the activation of C-H and more polar E-H bonds,[6a,f,7] and, in some cases, involvement in catalytic processes.[6a,b,7,8] To date, such TM-LA cooperativity has been dominated by cases where the LA is a B or Al center that is brought into proximity with the TM via a constrained geometry ligand, typically a bi- or polydentate P- or N-based species.[6−9] Herein, we report on the preparation and reactivity of a novel TM-LA system, $[Ru(IPr)_2(CO)ZnEt]BAr^F_4$ (**2**),[10] which features a direct, unsupported Ru-Zn bond and is accessed via the simple addition of $ZnEt_2$ to $[Ru(IPr)_2(CO)H]BAr^F_4$ (**1**).[11] Complex **2** can activate H_2 with net addition across the Ru-Zn bond to give $[Ru(IPr)_2(CO)(\eta^2\text{-}H_2)(H)_2ZnEt]BAr^F_4$ (**3**).[12] The observation of facile intramolecular H/H exchange in **3**, along with DFT calculations, highlights the ability of the TM-LA {Ru-Zn} moiety to act as a flexible and reversible hydride shuttle.

In line with the reported electrophilic reactivity of the hydride ligand in $[Ru(IPr)_2(CO)H]BAr^F_4$ (**1**),[11] addition of 1 equiv of $ZnEt_2$ to a fluorobenzene solution of this species gave the Ru-Zn complex **2** (Scheme 1), which was isolated as a red solid in 76% yield. ^{1}H NMR spectroscopy confirmed the absence of any hydride ligand in **2** as well as the presence of a single ZnEt group on the basis of the 8:3:2 ratio of ^{i}Pr methine protons to low-frequency signals at δ 0.73 (CH_3) and δ −0.11 (CH_2).

Upon shaking a C_6H_5F solution of **2** under H_2 (1 atm), there was an instantaneous color change (deep red to colorless)

Scheme 1. Formation and Reactivity of 2−4[a]

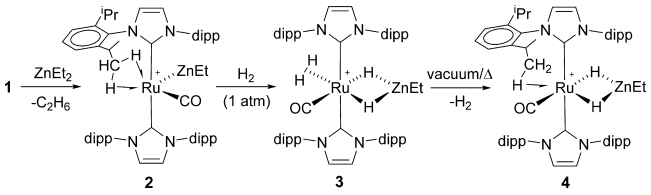

[a]dipp = 2,6-diisopropylphenyl. BAr^F_4 anions not shown.

resulting from the formation of the novel dihydrogen dihydride complex $[Ru(IPr)_2(CO)(\eta^2\text{-}H_2)(H)_2ZnEt]BAr^F_4$ (**3**, Scheme 1). The ^{1}H NMR spectrum of **3** exhibited two hydride resonances, a broad signal at δ −5.33 and a sharp peak at δ −12.13, in a relative ratio of 3:1. Cooling to −28 °C resolved the broad resonance into two signals (relative ratio 2:1) at δ −5.09 and −7.79 (with T_1 values of 31 and 72 ms, respectively),[13] assigned to Ru(η^2-H_2) and Ru-H-Zn (trans to CO), respectively. Both signals remained broad, indicative of exchange; this was confirmed by exchange spectroscopy (EXSY) and magnetization transfer experiments (Figure S11). No exchange with the remaining Ru-H-Zn trans to dihydrogen (δ −12.13, T_1 = 809 ms; T_1(min) = 638 ms (CD_2Cl_2, 400 MHz, −41 °C)) was found. However, upon exposure of **3** to 1 atm D_2, ^{1}H and ^{2}H NMR spectra showed unequivocally that all three sites underwent a slower chemical exchange, with deuterium incorporated into the Ru(η^2-H_2) and at both Ru-H-Zn positions.

The η^2-H_2 ligand in **3** proved hard to dissociate, with only ca. 20% conversion to $[Ru(IPr)_2(CO)(H)_2ZnEt]BAr^F_4$ (**4**) apparent, even after a C_6H_5F solution of **3** was evaporated to complete dryness. In fact, full conversion to **4** required heating a solid sample of **3** at 50 °C under dynamic vacuum for 24 h. Subjecting solid **3** to vacuum/heat for further time (ca. 72 h) showed that all four hydride ligands could be removed, although re-formation of **2** was also accompanied by additional, unidentified side products. Complex **4** displayed a low-frequency (δ −27.06) Ru-H-Zn signal, which now exchanged on the NMR time scale (magnetization transfer and EXSY measurements, Figure S12), with a second Ru-H-Zn resonance at δ −3.75.

The molecular structures of the cations in **2**, **3**, and **4** are shown in Figure 1, along with a comparison to computed data for the central {Ru(H)$_n$Zn} moieties in each case (n = 0, 4, and 2, respectively). **2** exhibits a Ru-Zn distance of 2.4069(7) Å[14] and

Received: May 21, 2016
Published: August 4, 2016

DOI: 10.1021/jacs.6b05243
J. Am. Chem. Soc. 2016, 138, 11081−11084

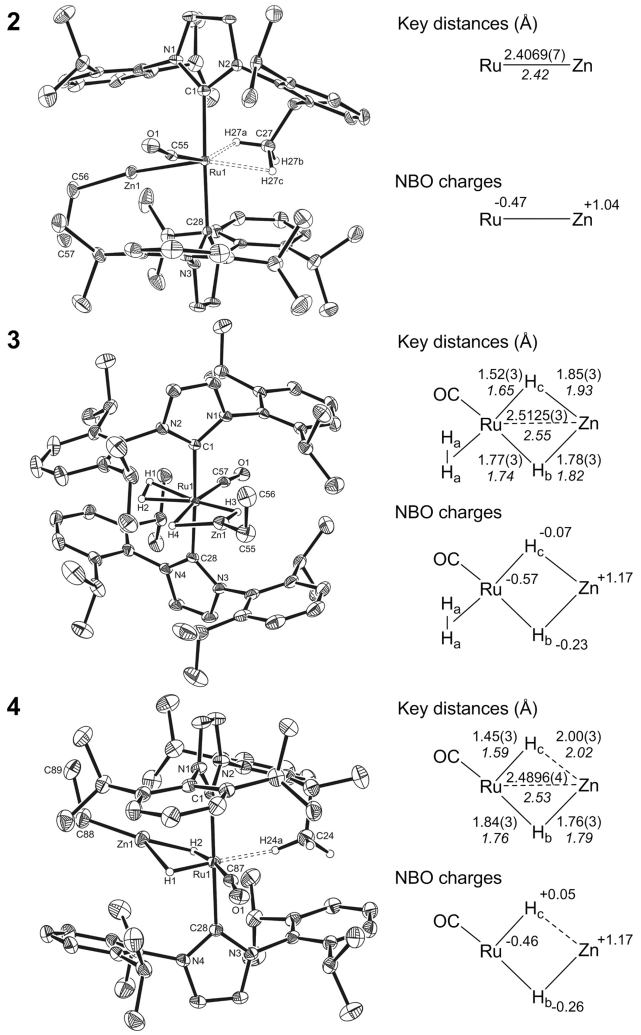

Figure 1. Molecular structures of the cations in **2**, **3**, and **4**. Thermal ellipsoids are shown at 30%. All non-hydride and non-agostic H-atoms are omitted for clarity. Also shown are comparisons of the key experimental and (in italics) computed distances around the central {Ru-Zn} moiety, along with the accompanying NBO charges.

also features two short Ru···H-C agostic interactions to one of the IPr ligands (Ru(1)···H(27A)-C(27), 2.13(3) Å; Ru(1)···H-(27C)-C(27), 2.31(4) Å), similar to those seen previously in **1**.[11] In **3** and **4**, the η^2-H_2 and hydride hydrogens were included in the model, the latter being refined without restraint. Both of these species have elongated Ru-Zn distances (2.5125(3) and 2.4896(4) Å, respectively) and have distinctly asymmetric {$Ru(H)_2Zn$} moieties that reflect the relative trans influences of the ligands completing the coordination sphere. Thus, the bridging hydrides trans to CO in **3** and **4** are approximately evenly shared between Ru and Zn, whereas the hydride trans to η^2-H_2 in **3** is significantly closer to Ru. This asymmetry is even more marked for the hydride trans to the agostic interaction in **4**.

DFT calculations[15] provide good absolute agreement for the Ru-Zn distances as well as the various Ru-H and Zn-H distances in **2**, **3**, and **4**, allowing for the inherent uncertainty in the H-atom positions (see Figure 1, right-hand side). NBO calculations characterize **2** as a Ru(0) species interacting with a cationic $\{ZnEt\}^+$ moiety via Ru→Zn σ-donation. In contrast, no significant direct Ru-Zn interaction is seen in either **3** or **4** (see Supporting Information for full details and orbital plots). NPA

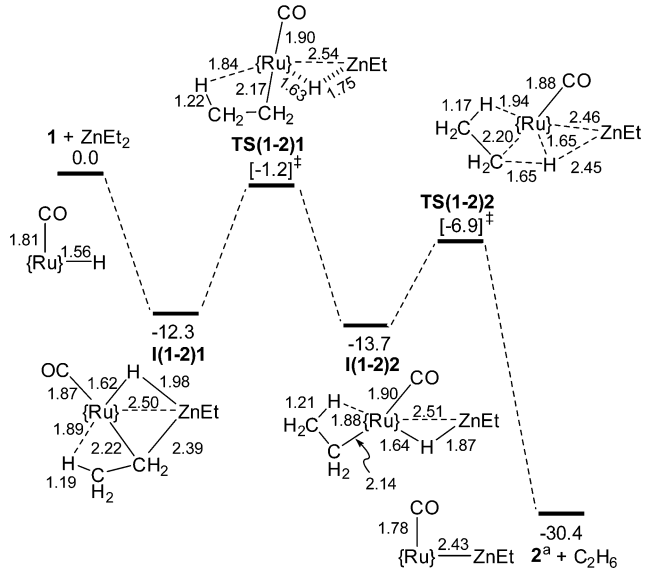

Figure 2. Computed reaction profile (free energy, kcal/mol) for the formation of **2** and C_2H_6 from **1** and $ZnEt_2$. Schematic structures show key distances (Å) within the equatorial plane; {Ru} = $Ru(IPr)_2^+$. An ethane σ-complex, **I(1-2)3**, generated from **TS(1-2)2** is omitted for clarity. [a]Non-agostic isomer of **2** located.

charges were used to characterize the nature of the hydride ligands. These indicate that the more evenly shared hydrides, H_b (trans to CO in **3** and **4**), exhibit a significant negative charge (q_H = −0.23 and −0.26, respectively), while this reduces and becomes positive as the hydride moves closer to Ru (H_c: q_H = −0.07 trans to η^2-H_2 in **3**; q_H = +0.05 trans to the agostic in **4**). For comparison, the terminal hydride in **1** (which lies trans to a vacant site) has q_H = +0.16. H_c in **4** therefore more resembles a terminal Ru-hydride. Indeed, an Atoms in Molecules study on **4** shows the absence of any Zn···H_c bond path (Figure S14).[16] The {$Ru(H)_2Zn$} moieties in these species are therefore structurally flexible and able to access both bridging and terminal hydride character, depending on the precise coordination environment.

Although examples of {$M(H)_nZn$} complexes exist for M = Ru,[17] as well as for other late TMs,[18] these all result from metal hydride precursors, and, to the best of our knowledge, formation via bimetallic M-Zn cleavage of H_2 has no precedent.[19,20] We have therefore used DFT calculations to study the formation of **2** as well as its onward reactivity with H_2 to **3** and **4**. Figure 2 indicates that the initial addition of $ZnEt_2$ to **1** forms an intermediate **I(1-2)1** at −12.3 kcal/mol in which the {Ru-Zn} moiety is bridged by both a hydride and an ethyl ligand; the latter also engages in a β-agostic interaction with the Ru center. Ethyl group transfer onto Ru proceeds via **TS(1-2)1** with a barrier of 11.1 kcal/mol and is induced by rotation of the {Ru(H)Zn} moiety, the movement of the bridging hydride below the equatorial coordination plane allowing the CO ligand to move trans to the developing Ru-Et ligand (**I(1-2)2**, −13.7 kcal/mol). The bridging hydride can now couple with the adjacent ethyl group via **TS(1-2)2** at −6.9 kcal/mol, leading, after release of ethane, to the formation of **2** at −30.4 kcal/mol. In this case, an alternative isomer of **2** devoid of agostic interactions is located, similar to the situation described previously for **1**, for which several isomers were also found.[11]

Figure 3 shows one possible mechanism for the reaction of **2** with H_2 to give **3** and **4**. Addition of two molecules of H_2 to **2** forms the bis-η^2-H_2 intermediate **I(2-3)1** at −32.1 kcal/mol. A very flat free energy surface then sees an essentially barrierless

DOI: 10.1021/jacs.6b05243
J. Am. Chem. Soc. 2016, 138, 11081−11084

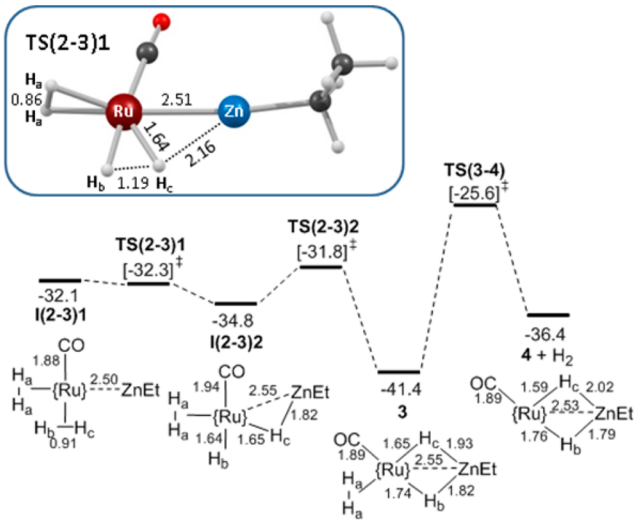

Figure 3. Computed reaction profile (free energy, kcal/mol) for the formation of **3** and **4** from **2**. Schematic structures show key distances (Å) within the equatorial plane, as well as the labeling scheme for the H-atoms; {Ru} = $Ru(IPr)_2^+$. Inset: Geometry of H_2 activation transition state **TS(2-3)1** (IPr ligands omitted).

cleavage of the H_b-H_c ligand, with net addition over the Ru-Zn bond to give **I(2-3)2** at −34.8 kcal/mol. Rotation about the Ru···Zn vector then allows transfer of H_b onto Zn to form **3** at −41.4 kcal/mol. H_2 loss from **3** is computed to be kinetically accessible ($\Delta G^{\ddagger}$ = 15.8 kcal/mol) but endergonic, **4** (+H_2) lying 5 kcal/mol above **3**. This is consistent with the observed reluctance of **3** to lose H_2.

The computed structure of the key H_2 activation transition state **TS(2-3)1** (inset, Figure 3) exhibits an elongated H_b-H_c moiety (1.19 Å, cf. 0.91 Å in **I(2-3)1**). At this point the Zn···H_c distance of 2.16 Å implies little, if any, interaction with the Zn center, and it is only after the cleavage that the Zn participates by accepting a hydride ligand. In addition, minimal polarization of the H_b-H_c bond is computed in the transition state (q_{Hb} = +0.05; q_{Hc} = +0.02). We therefore propose that H_2 activation occurs via oxidative cleavage mediated by Ru, followed by hydride transfer to Zn. In support of Ru being the key player in the H_2 cleavage, the activation of H_a-H_a trans to Zn in **I(2-3)1** was also characterized: this proceeds via a structurally similar transition state at −28.6 kcal/mol, which leads to a Ru(η^2-H_2)$(H)_2$ complex in which the Zn is unable to accept either hydride (Figure S17).

The mechanisms of H/H exchange in **3** and **4** have also been modeled. For **3**, exchange occurs between the η^2-H_2 ligand and the cis bridging hydride (H_a/H_b exchange) as well as between the two chemically distinct bridging hydrides (H_b/H_c exchange). H_b/H_c exchange can proceed via the mechanism in Figure 3, with reversible formation of the bis-η^2-H_2 complex **I(2-3)1** and rotation of the H_b-H_c ligand. The latter occurs via a transition state at −28.3 kcal/mol, giving an overall exchange barrier of 13.1 kcal/mol. For H_a/H_b exchange, a σ-CAM process[21] was characterized that sees formation of the H_a/(η^2-H_a-H_b) complex, **I(3-3′)** (Figure 4a). H_a-H_b rotation and reversal of the σ-CAM completes the exchange, the rotation transition state being the highest point in this process and equating to an overall barrier of 9.8 kcal/mol. The lower barrier for H_a/H_b exchange is consistent with the EXSY experiments indicating that only that process proceeded on the NMR time scale.[22] H_b/H_c exchange in **4** proceeds by a mechanism similar to that in **3** (Figure 4b). Thus, initial rotation about the Ru···Zn vector cleaves the Zn-H_b bond and forms **I(4-4′)1**; H_c

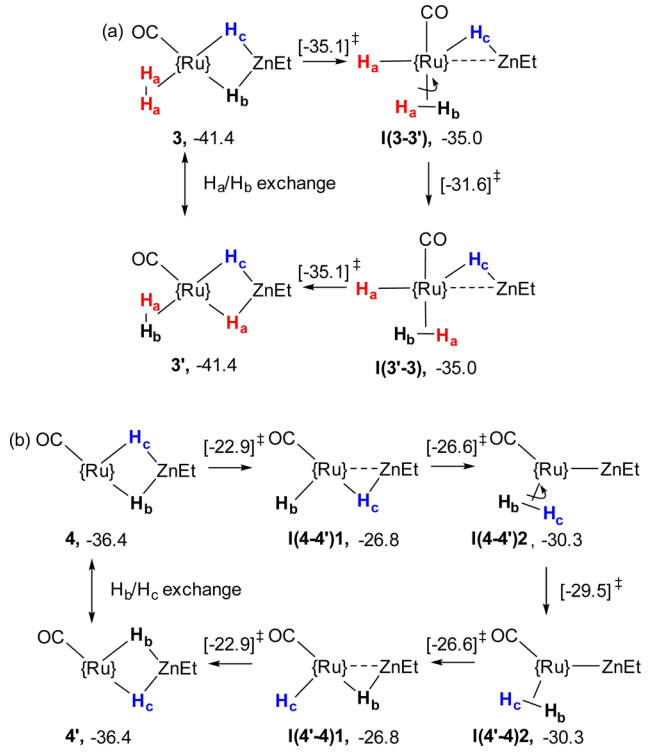

Figure 4. Computed mechanisms (free energy, kcal/mol) for (a) H_a/H_b in **3** and (b) H_b/H_c in **4**; {Ru} = $Ru(IPr)_2^+$. Transition-state energies for each step are given in square brackets.

can then transfer onto H_b to form the η^2-H_b-H_c complex **I(4-4′)2**. H_2 rotation and reversal of these processes complete the exchange. The highest transition states in this process are at −22.9 kcal/mol and correspond to an overall barrier of 13.5 kcal/mol. In principle, movement of the CO ligand from trans to H_b to trans to H_c would also render these two sites equivalent. However, this process has a barrier of 31.5 kcal/mol as it passes through a symmetrical Y-shaped {$RuCO(H)_2$} moiety, which is strongly disfavored for a d^6 configuration.[23]

To probe whether other E-H bonds could add across the Ru-Zn bond in **2**, preliminary investigations with both protic and hydridic reagents have been undertaken. NH_3 simply coordinated to form the ammonia complex [$Ru(IPr)_2(CO)(NH_3)$ZnEt]-BAr^F_4 (**5**, Figure S13). With HBcat and $PhSiH_3$, room-temperature dehydrogenation took place to give **3** as the major Ru-containing product of both reactions. Surprisingly, even a 1:1 ratio of **2**:HBcat generated hydride signals characteristic of **3**, suggesting that a strong driving force exists for formation of the {$Ru(H)_2$Zn} moiety. ^{11}B NMR spectroscopy confirmed the formation of B_2cat_2 (δ 31) but also showed a second major product at δ 22, consistent with the formation of B_2cat_3.[24] In the reaction of **2** with $PhSiH_3$, ^{29}Si NMR spectroscopy showed that Ph_3SiH and Ph_2SiH_2 were the major Si-containing reaction products, although a number of other, lower intensity signals were also present which we believe arise from the presence of three reactive Si-H bonds in the starting material, as well as the need for SiH_4 formation for atom balance. There is a clear silane dependence to this chemistry since no reaction was seen between **2** and either Ph_2SiH_2 or $PhMe_2SiH$. Further studies are required to elucidate the pathways of the borane/silane dehydrogenation reactions.

In conclusion, we have described the facile formation of a TM-LA heterobimetallic species, **2**, featuring an unconstrained and

DOI: 10.1021/jacs.6b05243
J. Am. Chem. Soc. 2016, 138, 11081−11084

unsupported Ru-Zn bond. This species is a rare example of an active TM-LA system derived from a non-group 13 element LA: **2** reacts directly with H_2 to form the $\{Ru(H)_2Zn\}$ species **3** and then **4**. DFT calculations indicate that H_2 activation proceeds via oxidative cleavage at Ru, with the adjacent Zn acting as a (reversible) hydride acceptor. H/H exchange experiments and calculations on **3** and **4** show that intermediates with unsupported Ru-Zn bonds retain kinetic accessibility even after H_2 addition. This, along with the observation of the activation of hydridic E-H bonds (E = B, Si), suggests that such unconstrained heterobimetallic TM-LA species may have potential applications in catalysis, and this possibility is being pursued in our laboratories.

■ ASSOCIATED CONTENT

Supporting Information

The Supporting Information is available free of charge on the ACS Publications website at DOI: 10.1021/jacs.6b05243.

Cartesian coordinates of all computed structures (XYZ)
Crystallographic data for **2**−**5** (CIF)
Synthesis, characterization, and computational data, including Figures S1−S23 and Tables S1−S4 (PDF)

■ AUTHOR INFORMATION

Corresponding Author

*s.a.macgregor@hw.ac.uk; m.k.whittlesey@bath.ac.uk

Notes

The authors declare no competing financial interest.

■ ACKNOWLEDGMENTS

We acknowledge financial support from the EPSRC (grant EP/J009962/1 for I.M.R.) and Heriot-Watt University (James Watt Scholarship to N.A.R.). We thank Prof. Ged Parkin for enlightening and very valuable discussions.

■ REFERENCES

(1) (a) Cooper, B. G.; Napoline, J. W.; Thomas, C. M. *Catal. Rev.: Sci. Eng.* **2012**, *54*, 1. (b) van der Vlugt, J. I. *Eur. J. Inorg. Chem.* **2012**, *2012*, 363. (c) Eisenstein, O.; Crabtree, R. H. *New J. Chem.* **2013**, *37*, 21. (d) Khusnutdinova, J. R.; Milstein, D. *Angew. Chem., Int. Ed.* **2015**, *54*, 12236. (e) Bouhadir, G.; Bourissou, D. *Chem. Soc. Rev.* **2016**, *45*, 1065.

(2) For LB = N, see: (a) Noyori, R.; Ohkuma, T. *Angew. Chem., Int. Ed.* **2001**, *40*, 40. (b) Sandoval, C. A.; Ohkuma, T.; Muñiz, K.; Noyori, R. *J. Am. Chem. Soc.* **2003**, *125*, 13490. (c) Maire, P.; Büttner, T.; Breher, F.; Le Floch, P.; Grützmacher, H. *Angew. Chem., Int. Ed.* **2005**, *44*, 6318. (d) Friedrich, A.; Drees, M.; Schmedt auf der Günne, J.; Schneider, S. *J. Am. Chem. Soc.* **2009**, *131*, 17552.

(3) For LB = O or S, see: (a) Sweeney, Z. K.; Polse, J. L.; Bergman, R. G.; Andersen, R. A. *Organometallics* **1999**, *18*, 5502. (b) Linck, R. C.; Pafford, R. J.; Rauchfuss, T. B. *J. Am. Chem. Soc.* **2001**, *123*, 8856. (c) Sellmann, D.; Prakash, R.; Heinemann, F. W.; Moll, M.; Klimowicz, M. *Angew. Chem., Int. Ed.* **2004**, *43*, 1877. (d) Ohki, Y.; Sakamoto, M.; Tatsumi, K. *J. Am. Chem. Soc.* **2008**, *130*, 11610. (e) Matsumoto, T.; Nakaya, Y.; Itakura, N.; Tatsumi, K. *J. Am. Chem. Soc.* **2008**, *130*, 2458. (f) Klare, H. F. T.; Oestreich, M.; Ito, J.; Nishiyama, H.; Ohki, Y.; Tatsumi, K. *J. Am. Chem. Soc.* **2011**, *133*, 3312.

(4) Gunanathan, C.; Milstein, D. *Acc. Chem. Res.* **2011**, *44*, 588.

(5) For early work on TM-LA complexes, see: (a) St Denis, J. N.; Butler, W.; Glick, M. D.; Oliver, J. P. *J. Organomet. Chem.* **1977**, *129*, 1. (b) Burlitch, J. M.; Leonowicz, M. E.; Petersen, R. B.; Hughes, R. E. *Inorg. Chem.* **1979**, *18*, 1097. For recent, pertinent reviews, see: (c) Amgoune, A.; Bourissou, D. *Chem. Commun.* **2011**, *47*, 859. (d) Maity, A.; Teets, T. S. *Chem. Rev.* **2016**, *116*, 8873.

(6) (a) Harman, W. H.; Peters, J. C. *J. Am. Chem. Soc.* **2012**, *134*, 5080. (b) Lin, T. P.; Peters, J. C. *J. Am. Chem. Soc.* **2013**, *135*, 15310. (c) Zeng, G.; Sakaki, S. *Inorg. Chem.* **2013**, *52*, 2844. (d) Harman, W. H.; Lin, T.-P.; Peters, J. C. *Angew. Chem., Int. Ed.* **2014**, *53*, 1081. (e) Cowie, B. E.; Emslie, D. J. H. *Chem. - Eur. J.* **2014**, *20*, 16899. (f) Barnett, B. R.; Moore, C. E.; Rheingold, A. L.; Figueroa, J. S. *J. Am. Chem. Soc.* **2014**, *136*, 10262. (g) Devillard, M.; Bouhadir, G.; Bourissou, D. *Angew. Chem., Int. Ed.* **2015**, *54*, 730. (h) Li, Y.; Hou, C.; Jiang, J.; Zhang, Z.; Zhao, C.; Page, A. J.; Ke, Z. *ACS Catal.* **2016**, *6*, 1655. (i) Devillard, M.; Declercq, R.; Nicolas, E.; Ehlers, A. W.; Backs, J.; Saffon-Merceron, N.; Bouhadir, G.; Slootweg, J. C.; Uhl, W.; Bourissou, D. *J. Am. Chem. Soc.* **2016**, *138*, 4917.

(7) (a) Fong, H.; Moret, M.-E.; Lee, Y.; Peters, J. C. *Organometallics* **2013**, *32*, 3053. (b) MacMillan, S. N.; Harman, W. H.; Peters, J. C. *Chem. Sci.* **2014**, *5*, 590. (c) Nesbit, M. A.; Suess, D. L. M.; Peters, J. C. *Organometallics* **2015**, *34*, 4741.

(8) (a) Tsoureas, N.; Kuo, Y.-Y.; Haddow, M. F.; Owen, G. R. *Chem. Commun.* **2011**, *47*, 484. (b) Cammarota, R. C.; Lu, C. C. *J. Am. Chem. Soc.* **2015**, *137*, 12486.

(9) (a) Bontemps, S.; Bouhadir, G.; Gu, W.; Mercy, M.; Chen, C.-H.; Foxman, B. M.; Maron, L.; Ozerov, O. V.; Bourissou, D. *Angew. Chem., Int. Ed.* **2008**, *47*, 1481. (b) Sircoglou, M.; Bontemps, S.; Bouhadir, G.; Saffon, N.; Miqueu, K.; Gu, W.; Mercy, M.; Chen, C.-H.; Foxman, B. M.; Maron, L.; Ozerov, O. V.; Bourissou, D. *J. Am. Chem. Soc.* **2008**, *130*, 16729. (c) Rudd, P. A.; Liu, S.; Gagliardi, L.; Young, V. G.; Lu, C. C. *J. Am. Chem. Soc.* **2011**, *133*, 20724. (d) Cowie, B. E.; Tsao, F. A.; Emslie, D. J. H. *Angew. Chem., Int. Ed.* **2015**, *54*, 2165.

(10) IPr = 1,3-bis(2,6-diisopropylphenyl)imidazol-2-ylidene; BAr^F_4 = $B\{C_6H_3(3,5\text{-}CF_3)_2\}_4^-$.

(11) Riddlestone, I. M.; McKay, D.; Gutmann, M. J.; Macgregor, S. A.; Mahon, M. F.; Sparkes, H. A.; Whittlesey, M. K. *Organometallics* **2016**, *35*, 1301.

(12) For a recent review of molecular Zn-H complexes, see: Wiegand, A.-K.; Rit, A.; Okuda, J. *Coord. Chem. Rev.* **2016**, *314*, 71.

(13) In CD_2Cl_2 (−28 °C), T_1 = 47 ms for the Ru-H-Zn resonance at δ −7.79. See SI.

(14) (a) Cadenbach, T.; Bollermann, T.; Gemel, C.; Tombul, M.; Fernandez, I.; von Hopffgarten, M.; Frenking, G.; Fischer, R. A. *J. Am. Chem. Soc.* **2009**, *131*, 16063. (b) Bollermann, T.; Gemel, C.; Fischer, R. A. *Coord. Chem. Rev.* **2012**, *256*, 537.

(15) Calculations were run with the Gaussian programs employing the BP86 functional. Free energies include corrections for fluorobenzene solvent and dispersion effects. See SI for references and full details, as well as functional testing.

(16) As the nature of the hydrides in the $\{Ru(H)_2Zn\}$ moiety is ambiguous, we did not adopt the half-arrow formalism of Parkin et al.: Green, J. C.; Green, M. L. H.; Parkin, G. *Chem. Commun.* **2012**, *48*, 11481.

(17) (a) Ohashi, M.; Matsubara, K.; Iizuka, T.; Suzuki, H. *Angew. Chem., Int. Ed.* **2003**, *42*, 937. (b) Ohashi, M.; Matsubara, K.; Suzuki, H. *Organometallics* **2007**, *26*, 2330. (c) Plois, M.; Hujo, W.; Grimme, S.; Schwickert, C.; Bill, E.; de Bruin, B.; Pöttgen, R.; Wolf, R. *Angew. Chem., Int. Ed.* **2013**, *52*, 1314. (d) Molon, M.; Gemel, C.; Fischer, R. A. *Eur. J. Inorg. Chem.* **2013**, *2013*, 3616. (e) Plois, M.; Wolf, R.; Hujo, W.; Grimme, S. *Eur. J. Inorg. Chem.* **2013**, *2013*, 3039.

(18) (a) Geerts, R. L.; Huffman, J. C.; Caulton, K. G. *Inorg. Chem.* **1986**, *25*, 590. (b) Fryzuk, M. D.; McConville, D. H.; Rettig, S. J. *Organometallics* **1993**, *12*, 2152. (c) Ekkert, O.; White, A. J. P.; Toms, H.; Crimmin, M. R. *Chem. Sci.* **2015**, *6*, 5617.

(19) For examples of Zn-H bond formation by activation of H_2, see: (a) Jochmann, P.; Stephan, D. W. *Angew. Chem., Int. Ed.* **2013**, *52*, 9831. (b) Jochmann, P.; Stephan, D. W. *Chem. Commun.* **2014**, *50*, 8395.

(20) Fafard, C. M.; Chen, C.-H.; Foxman, B. M.; Ozerov, O. V. *Chem. Commun.* **2007**, 4465.

(21) Perutz, R. N.; Sabo-Etienne, S. *Angew. Chem., Int. Ed.* **2007**, *46*, 2578.

(22) A pathway linking **I(2-3)2** (Figure 3) to **I(3-3′)** (Figure 4a) was also characterized and provides an alternative route from **2** to **3** via a transition state at −31.2 kcal/mol (see Figure S18).

(23) Riehl, J.-F.; Jean, Y.; Eisenstein, O.; Pélissier, M. *Organometallics* **1992**, *11*, 729.

(24) Westcott, S. A.; Blom, H. P.; Marder, T. B.; Baker, R. T.; Calabrese, J. C. *Inorg. Chem.* **1993**, *32*, 2175.

DOI: 10.1021/jacs.6b05243
J. Am. Chem. Soc. 2016, 138, 11081−11084